Nucleobase sensing using highly-sensitive surface-enhanced Raman spectroscopy templates comprising organic semiconductor peptide nanotubes and metal nanoparticles

Sawsan Almohammed [a, b], Brian J. Rodriguez * [a, b], James H. Rice * [a]

[a]School of Physics, University College Dublin, Belfield, Dublin 4, Ireland
[b]Conway Institute of Biomolecular and Biomedical Research, University College Dublin, Belfield, Dublin 4, Ireland

*Corresponding authors: brian.rodriguez@ucd.ie and james.rice@ucd.ie

Abstract

Templates formed from aligned diphenylalanine nanotubes with plasmon-active metal nanoparticles are a promising nanocomposite for large-scale, rapid, stable, and cost-effective surface-enhanced Raman spectroscopy (SERS) substrates. The high sensitivity of such templates arises from an arrangement of densely packed plasmon-active silver nanoparticles that enhance the localized electromagnetic field and allow the detection of the nucleobases adenine, cytosine, thymine, uracil, and guanine at concentrations in the range 10^{-5} to 10^{-9} M. Blinking of the SERS signal is observed, indicating sensitivity down to the single or few molecule limit. Such blinking could result from charge transfer processes. These results demonstrate the potential for using aligned diphenylalanine nanotube-metal nanoparticle templates for practical monitoring of biomolecules and are promising initial steps toward the use of peptide nanotube-based templates in diagnostic sensing applications.

Keywords: diphenylalanine nanotubes; nucleobases; surface-enhanced Raman spectroscopy; nanocomposites; self-assembly; organic template

Introduction

Developments in materials science have produced a range of optically-active materials.[1–7] Self-assembly of bioinspired building blocks into well-ordered nanostructures has emerged as an attractive route for the development of advanced nanocomposite materials with unique physical and chemical properties.[6,7] One of the most promising building blocks is the aromatic dipeptide diphenylalanine (FF), the core recognition motif of the amyloid beta peptide. FF can self-assemble into nano- or micro-sized structures such as FF peptide nanotubes (FF-PNTs). FF-PNTs have been shown to possess remarkable physical and chemical stability and possess unique mechanical,[8,9] electrical,[10,11] and optical properties.[12,13] FF-PNTs are also piezoelectric,[10,11] pyroelectric, and biocompatible.[14–16] For these reasons, FF-PNTs have been the focus of extensive scientific attention for their use in catalysis,[14–16] energy harvesting,[17] and biosensing applications.[18–22]

One Raman-based biosensing application utilizes composites of FF-PNTs and plasmonic metal nanoparticles. These composites can be used to provide a chemical fingerprint of an analyte molecule at different concentrations.[6,7] Generally, Raman scattering cross-sections from analyte molecules are weak, making the detection of such molecules difficult to obtain at low

concentrations. However, surface-enhanced Raman spectroscopy (SERS) greatly increases the Raman signal strength. This enhancement results from an intense local amplification of the electric field near a metal surface when the surface plasmon resonates in-phase with the incident light.[23,24] These regions are called electromagnetic "hot spots", which can enable the detection of molecules using Raman down to the single molecule level.[23,24] A commonly used approach to achieve single molecule SERS is to use aggregated metal colloids that can be obtained by changing the solvent or the ionic strength.[23,24] However, both the size and the geometry of the resulting aggregate can be difficult to control. Challenges in controlling the arrangement and location of plasmon-active metal nanoparticles, as well as their stability, sensitivity, and biocompatibility, frequently limit practical applications of SERS.[25,26]

Nanocomposites based on plasmon-active metal nanoparticles and self-assembled organic templating materials offer attractive opportunities to achieve controlled metal nanoparticle localization, which can potentially improve SERS signal reproducibility, stability, and sensitivity.[18–22,25–28] We have previously reported that FF-PNT-based templates can provide control over metal nanoparticle distributions, resulting in the formation of a large number electromagnetic "hot spots" and enhanced SERS sensitivity, allowing the detection of analyte molecules/dyes (such as porphyrin, amino nitrophenol, and rhodamine B) with concentrations as low as 10^{-15} M.[6,7]

To examine the potential of FF-PNT/Ag NP templates for probing biological molecules, we investigated in this study non-resonant SERS spectra of the nucleobases adenine, guanine, cytosine, thymine, and uracil at concentrations ranging from 10^{-5} to 10^{-10} M. We found that the template produces a strongly-enhanced Raman signal from all nucleobases compared to control samples consisting solely of Ag NPs. The high sensitivity of such templates arises from: firstly, the ability of the template to densely arrange plasmon-active Ag NPs that enhance the localized electromagnetic field; secondly, the wettability of the template or the chemical interaction with the nanotubes that facilitates the spreading of the analyte; thirdly, the charge transfer process between Ag NPs with FF-PNTs (due to different work function) that enhances the chemical mechanism in SERS. Nucleobases are challenging molecules to detect using SERS due to their low Raman cross-sections.[29–32] Up to now, studies reporting the detection of nucleobases typically used advanced methods, such as tip-enhanced Raman spectroscopy, which allowed the detection of nucleobases at concentrations of 10^{-5} M.[29–33] The stability of the FF-PNT/Ag NP template was tested by comparing SERS intensity over a period of one month and by using different laser powers in the range of 5 – 50 mW, appropriate for biomolecules.[29–33] The SERS intensity decreased by around 6% over 1 month, demonstrating the high stability of the template. Being able to detect nucleobases at relatively low concentrations with high stability is advantageous for biomolecular sensing and demonstrates the high-sensitivity of FF-PNT/Ag NP templates.[29–33] The biocompatibility, ease of preparation, and stability of this organic template could potentially widen the use of FF-PNT/Ag NP templates as a biosensor for monitoring biomolecule interactions.

Experimental Section

Preparation of FF-PNT Solution

FF-PNTs were prepared by dissolving L-diphenylalanine peptide (Bachem, Bubendorf, Switzerland) in 1,1,1,3,3,3-hexafluoro-2-propanol (Sigma-Aldrich, Ireland) at an initial concentration of 100 mg/ml, which was then further diluted in deionized water to a final

concentration of 2 mg/ml for FF-PNTs to self-assemble. Fresh stock solutions were prepared for each experiment.

Preparation of Nucleobase Solutions

To prepare thymine (T0376, Sigma-Aldrich), cytosine (C3506, Sigma-Aldrich), uracil (U0750, Sigma-Aldrich), adenine (A8626, Sigma-Aldrich), and guanine (G11950, Sigma-Aldrich) solutions, nucleobase powder from each molecule was diluted with deionized water to a final concentration of 10^{-4} M, then stirred for around 30 minutes using a magnetic stirrer until the powder dissolved. The solution was further diluted with deionized water to a range of concentrations, from 10^{-5} to 10^{-10} M.

UV-Vis Absorbance Spectrometer

Optical absorbance measurements of FF-PNTs with and without Ag NPs and nucleobase (thymine, cytosine, uracil, adenine, and guanine) were performed on an UV-Vis absorbance spectrometer (V-650, JASCO, Inc.) under identical settings: 1 nm step size, 1 nm bandwidth, and 400 nm/min scan speed across a 190–900 nm range. A quartz cuvette or glass cover slip was used to conduct the measurements. Concentrations of 10^{-5} M were used.

Preparation of Si Substrate

Si wafers (Si Mat), cut to 2 cm x 1 cm were immersed in acetone for 2 minutes and then washed with ethanol and isopropanol (Sigma-Aldrich). Deionized water was used to rinse the substrates, which were then blown dry using compressed nitrogen. A 0.5 cm wide hydrophilic region was created on the Si surface using UV/ozone exposure through a physical mask to facilitate the preparation of an aligned FF-PNT template as described previously.[6,7]

Preparation of FF-PNT/Ag NP Template

FF-PNT/Ag NP templates were prepared using 2 mg/ml of FF solution heated at 100°C for 2 minutes and Ag NPs (795968, Sigma-Aldrich) with a diameter of 50 nm and a concentration of 0.02 mg/ml in water. 20 µl of Ag NP solution was added to 60 µl of the heated FF solution and stirred for 3 minutes. 30 µl of the mixed solution was then deposited on the UV/ozone-exposed Si substrate to create the aligned FF-PNT/Ag NP template. To deposit Ag NPs on a Si substrate, 20 µl of Ag NPs (0.02 mg/ml) was diluted in 60 µl of water. Then 30 µl of the solution was deposited on Si substrate.

Scanning Electron Microscopy

Scanning electron microscopy (SEM) (JSM-7600F, JEOL, operated at 5 kV) was employed to characterize and observe the location of NPs decorating the surface. SEM imaging was also undertaken for the FF-PNT/Ag NP template after the addition of the nucleobase. A thin (~ 8 nm) layer of gold was sputtered on the samples before SEM imaging (Hummer IV, Anatech USA).

Raman Spectroscopy

SERS measurements were performed using a bespoke Raman system (IX71, Olympus) comprising a monochromatic green laser (532 nm, 8 mW incident power, ThorLabs) with beam splitter and long pass filter (RazorEdge, Semrock), a spectrograph (SP-2300i, Princeton Instruments), and a CCD camera (IXON, Andor). A 50x objective was used to focus the laser. Raman spectra were collected with an exposure time of 1 s. 60 µl of all nucleobases at different concentrations were deposited separately above the aligned FF-PNT/Ag NP template. The average of 10 measurements is reported. Typically, the average of 10 measurements from one

location on the same sample is reported; however, the spatial variability is assessed as the average of 10 spectra recorded from different locations.

Results and Discussion

Raman scattering from FF-PNT/Ag NP templates with the nucleobases adenine, guanine, cytosine, thymine, and uracil at different concentrations, from 10^{-5} to 10^{-9} M, was recorded to demonstrate the sensitivity of the template as a SERS-active platform for biomolecule detection, as shown schematically in Fig. 1a. The process to form aligned FF-PNTs with Ag NPs followed a previously reported method.[6,7] Briefly, hydrophilic regions were created by growing a silicon oxide layer on an Si surface via UV/ozone exposure through a Si mask with an opening of 0.5 cm. The difference in wettability between regions leads to a chemical force that results in the alignment of the FF-PNTs and the formation of the FF-PNT/Ag NP composite template.[6,7] SEM images of the resulting template are shown in Fig. 1b. The FF-PNTs are hollow (Fig. 1b, inset) with an average outer diameter of 3.4 ± 1.2 μm determined from measurements of 20 FF-PNTs. SEM images show small spherical features that are assigned to Ag NPs as small and large clusters located on and between the FF-PNTs, as previously reported.[6,7] Enhanced Raman scattering is expected from nucleobases in proximity to the NPs, as shown schematically for thymine in Fig. 1c. For Raman measurements, an excitation wavelength of 532 nm was used that is non-resonant with the nucleobases, which possess absorption bands in the ultraviolet region (< 350 nm) (Fig. 1d).

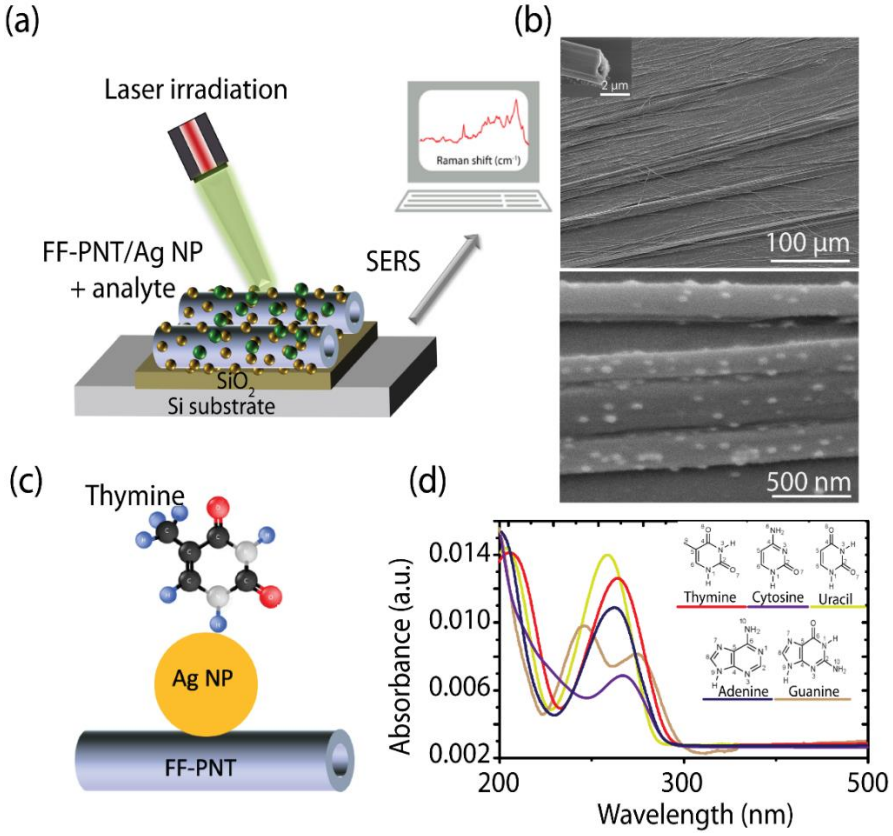

Figure 1. *(a) Illustration of SERS measurements of an aligned FF-PNT/Ag NP template with analyte molecule (nucleobase). (b) SEM images of the template; a hollow FF-PNT is shown in inset. (c) Schematic showing a thymine molecule on an Ag NP on an FF-PNT. (d) Absorption spectra of nucleobases thymine (red), cytosine (purple), uracil (light green), adenine (blue), and guanine (light brown).*

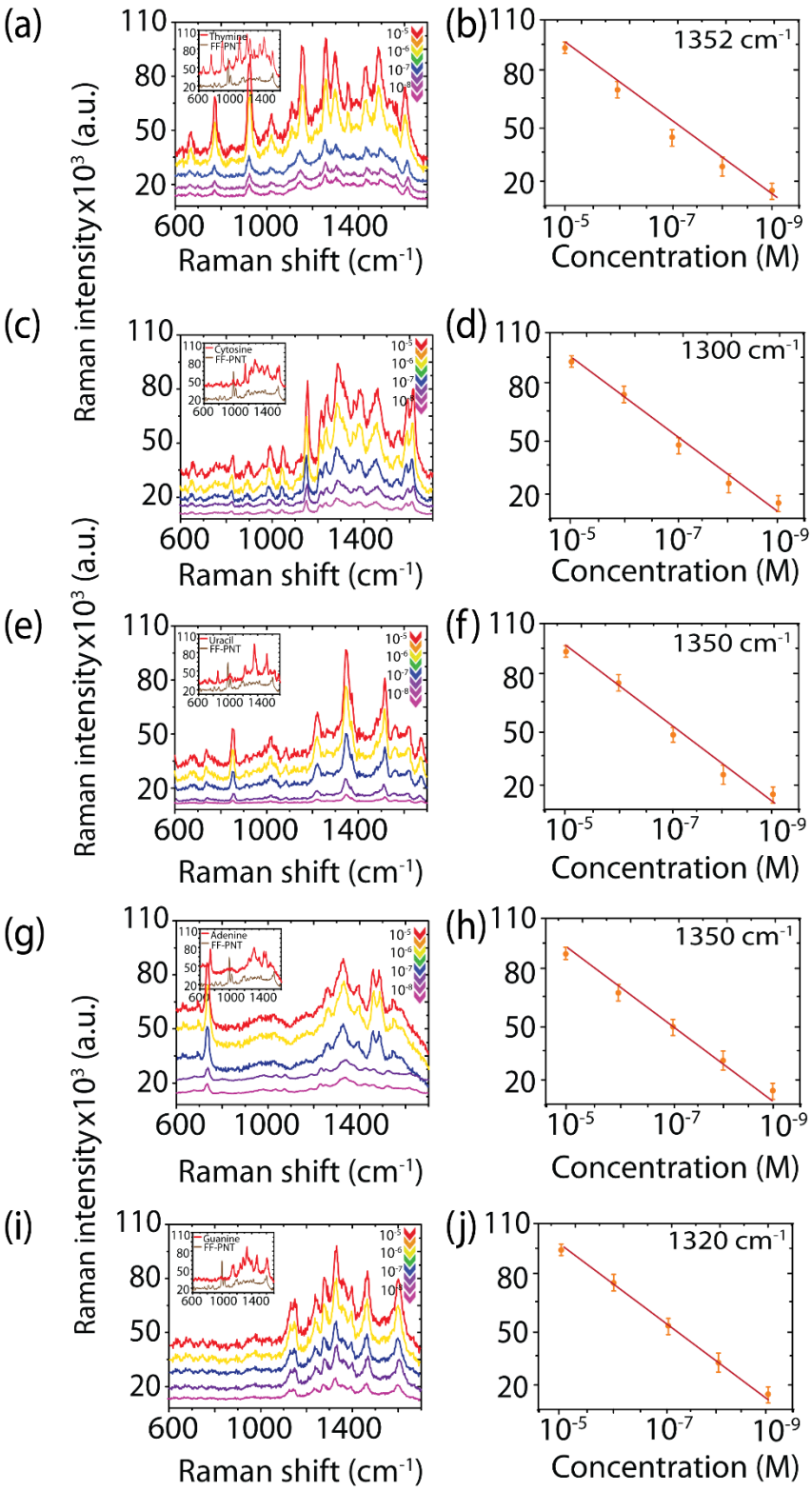

Figure 2. *SERS measurements of aligned FF-PNT/Ag NP templates in the presence of nucleobases. SERS spectra at different concentrations from 10^{-5} to 10^{-9} M for (a) thymine, (c) cytosine, (e) uracil, (g) adenine, and (i) guanine. Insets in each panel show the Raman spectra for the nucleobase (red) and FF-PNT (brown). Plot of concentration versus intensity for bands at (b) 1352 cm^{-1} for thymine, (d, f) 1300 cm^{-1} for cytosine and uracil, respectively, (h) 1350 cm^{-1} for adenine, and (j) 1320 cm^{-1} for guanine. The plots (b, d, f, h, j) were fitted using a linear fit.*

SERS spectra of thymine recorded at concentrations from 10^{-5} to 10^{-9} M on the FF-PNT/Ag NP template are shown in Fig. 2a. Peaks from the thymine nucleobase, such as bands at 1470 cm^{-1} (CH_3 bending), 1397 cm^{-1} (N_1–H bending, N_3–H), 1221 cm^{-1} (C_5–C_9), and 785 cm^{-1} (ring breathing mode) dominate the SERS spectra at nucleobase concentrations of 10^{-5} and 10^{-6} M (Fig. 2a). The SERS spectra of thymine and FF-PNT/Ag NP template (Fig. 2a, inset) possess different spectral features, enabling them to be distinguished from each other. The FF-PNT template possesses features in agreement with those reported in the literature, such as an aromatic ring breathing mode at 1002 cm^{-1} and a phenyl vibrational band at 1603 cm^{-1}.[6,7,34] At relatively low concentrations of thymine (10^{-7} and 10^{-8} M), fewer bands (e.g., 998, 1000, 1035, 1098, 1279, 1352, 1397, and 1605 cm^{-1}) arising from thymine are observed as the overall signal decreases (Fig. 2a). This decrease is apparent when plotting the intensity for the 1352 cm^{-1} band as a function of nucleobase concentration (Fig. 2b). The plot shows a linear decrease in SERS peak intensity as the concentration is lowered from 10^{-5} to 10^{-9} M.

SERS spectra of cytosine (Fig. 2c) were recorded at different concentrations from 10^{-5} to 10^{-9} M on the FF-PNT/Ag NP template. The intensity for the cytosine band at 1330 cm^{-1} decreased linearly as the concentration was lowered from 10^{-5} to 10^{-9} M (Fig. 2d). Cytosine is reportedly a difficult molecule to detect using SERS due to the low stability of hydroxylamine-reduced Ag NPs in the presence of cytosine.[29–33] Madzharova et al.[29] detected cytosine using hyper Raman spectroscopy (SEHRS) with a SERS-active substrate. In our study, we have successfully detected all reported cytosine bands, including bands at 1591 cm^{-1} (NH_2 bending), 1544 cm^{-1} (N_3–C_4–C_5), 1422 cm^{-1} (N_1–H, C_5–H, C_6–H), 1228 cm^{-1} (C–N), and 1038 cm^{-1} (ring breathing mode), using the FF-PNT/Ag NP template. The modes recorded in our study are in line with what has been reported in literature using SEHRS and density functional theory (DFT) analysis.[29–33]

Previous SERS, SEHRS, and DFT studies have reported that pyrimidine bases (thymine and cytosine) can interact with Ag NP surfaces in their deprotonated forms, even at a neutral pH.[29–33] Under the conditions of the experiments performed here, the SERS spectra of thymine and cytosine (Fig. 2a,c) arise from the anions of the two nucleic acid bases. In our case, the strong signal recorded for thymine at 1600 cm^{-1} (C=O stretching vibrations) and 785 cm^{-1} (ring breathing mode) are in good agreement with the results recorded using SEHRS, noting that these bands were not detected in previous SERS studies undertaken at a neutral pH.[29–33] The SERS band arising from thymine (on FF-PNT/Ag NP) at 1520 cm^{-1}, which is assigned to a ring stretching mode, possesses a strong SERS intensity in the current study. In comparison, when using the SEHRS technique, the intensity for this specific mode was weak. A band at around 935 cm^{-1} was observed for thymine using the FF-PNT/Ag NP template that possesses a strong SERS band intensity assigned to the out of plane wagging N_1–H, N_3–H modes that are not detectible using SEHRS, but were found by DFT analysis.[29–33] Regarding cytosine, the most obvious difference between SERS from the FF-PNT/Ag NP template and SEHRS is that the wagging C_6–H mode at 920 cm^{-1} was not detectible using SEHRS. However, there is good similarity for the reported SEHRS spectra and the SERS spectra reported here (Fig. 2c) for the remaining modes, especially the two bands at 1307 cm^{-1} (ring stretching C–N) and a relatively strong NH_2 bending mode at 1590 cm^{-1}, which both possess strong Raman intensities.[29–33]

The high SERS signal from the nucleobase (thymine and cytosine) observed using the FF-PNT/Ag NP template can be attributed to FF-PNTs supporting the formation of areas consisting of dense concentrations of Ag NPs. [6,7] This results in "hot-spots" with highly localized electromagnetic fields that enhance the SERS signal, as noted previously.[6,7] Another possible

reason for the high sensitivity of the template could be attributed to enhancement of the charge transfer process with analyte molecule. The difference between the Fermi level of the aligned FF-PNTs (6.2 eV below the vacuum level[6,7]) and the lowest unoccupied molecular orbital is 2.2 eV,[35] which is less than the laser excitation (532 nm; 2.3 eV). Therefore, it is possible that the excitation facilitates charge transfer from the aligned FF-PNT/Ag NP template to nucleobase molecules, and hence enhances the SERS signal.[6,7,35]

The SERS spectra of uracil, adenine, and guanine at different concentrations from 10^{-5} to 10^{-9} M on the FF-PNT/Ag NP template (Fig. 2e, g, and i) were also in good agreement with literature.[29–33] As with thymine and cytosine, SERS signal intensity decreased linearly with decreasing concentration (Fig. 2f, h and j). Previously, a low intensity ring breathing band for uracil at 802 cm^{-1} was detected by SEHRS but not by SERS.[33] This band and other low intensity bands located at 643, 700, and 720 cm^{-1} were detected using the aligned FF-PNT/Ag NP template. Moreover, a strong band located at 1320 cm^{-1} was identified that was not detectable or was low in signal intensity when measured using SEHRS.[33] The strong bands recorded for uracil at 1489 cm^{-1} (stretching C_6–N_1, C_4–C_5, C_2=O) and 1630 cm^{-1} (stretching C_2=O, C_4=O, N_1–H bending, C_5–H) in our experiment are in line with what has been reported in literature using SEHRS and other SERS measurements based on reduced Ag NPs.[29–33] For adenine, the most difficult bands to detect are reportedly at 691, 960, 1095, 1398, and 1641 cm^{-1} with the symmetric ring breathing mode (734 cm^{-1}) often dominating the SERS spectra of adenine; however, DFT and theoretical studies have proved that these modes are attributed to the adenine nucleobase.[29–33] In our system, these bands were observed at concentrations of 10^{-5} and 10^{-6} M (Fig. 2g). While for concentrations from 10^{-7} to 10^{-9} all reported SERS bands are seen, expect the vibration bands at 619, 1600, and 1641 cm^{-1}. Furthermore, the SERS data collected from the FF-PNT/Ag NP template indicate a strong contribution from several bands associated with NH_2 and N_9–H deformation modes, specifically the NH_2 rocking band at 1026 cm^{-1} and the in-plane NH_2 scissoring vibrations at 1487, 1551, and around 1641 cm^{-1}, in good agreement with adenine bands observed using SEHRS.[29–33] For guanine, a strong ring breathing mode at 660 cm^{-1} was observed (Fig. 2i). Additional bands at 950, 1016, 1570, and 1646 cm^{-1}, were also detected, in agreement with previous SEHRS studies.[29–33]

In general, studies have found that the SERS spectra of nucleobases are dominated by in-plane vibrational modes (from ~ 1653 to 920 cm^{-1}).[29–33] It can be concluded that the orientation of, for example, adenine should be perpendicular to the Ag NPs surface due to the decreased intensity of the vibrational modes involving the nitrogen atoms N_1, N_3 and N_9 as well as the preferentially enhanced SERS signals of Raman modes involving the external amino group and the nitrogen atom N_7.[29–33] In this scenario, the interaction between adenine and the Ag NPs occur via the external amino group and N_7.[29–33] Furthermore, studies have suggested that out-of-plane modes appear weakened in the SERS spectra but do not disappear completely. In our case, the out-of-plane modes (~ 764, 689 and 564 cm^{-1}) were strong and distinguishable in SERS spectra. FF-PNTs consist of carbonyl and amino functional groups that may facilitate interactions with the nucleobases,[10,11,18–20] aiding out-of-plane modes in the SERS spectra. In addition, nucleobase molecules aggregate on and between FF-PNTs (Fig. 3) likely as a result of drying effects.

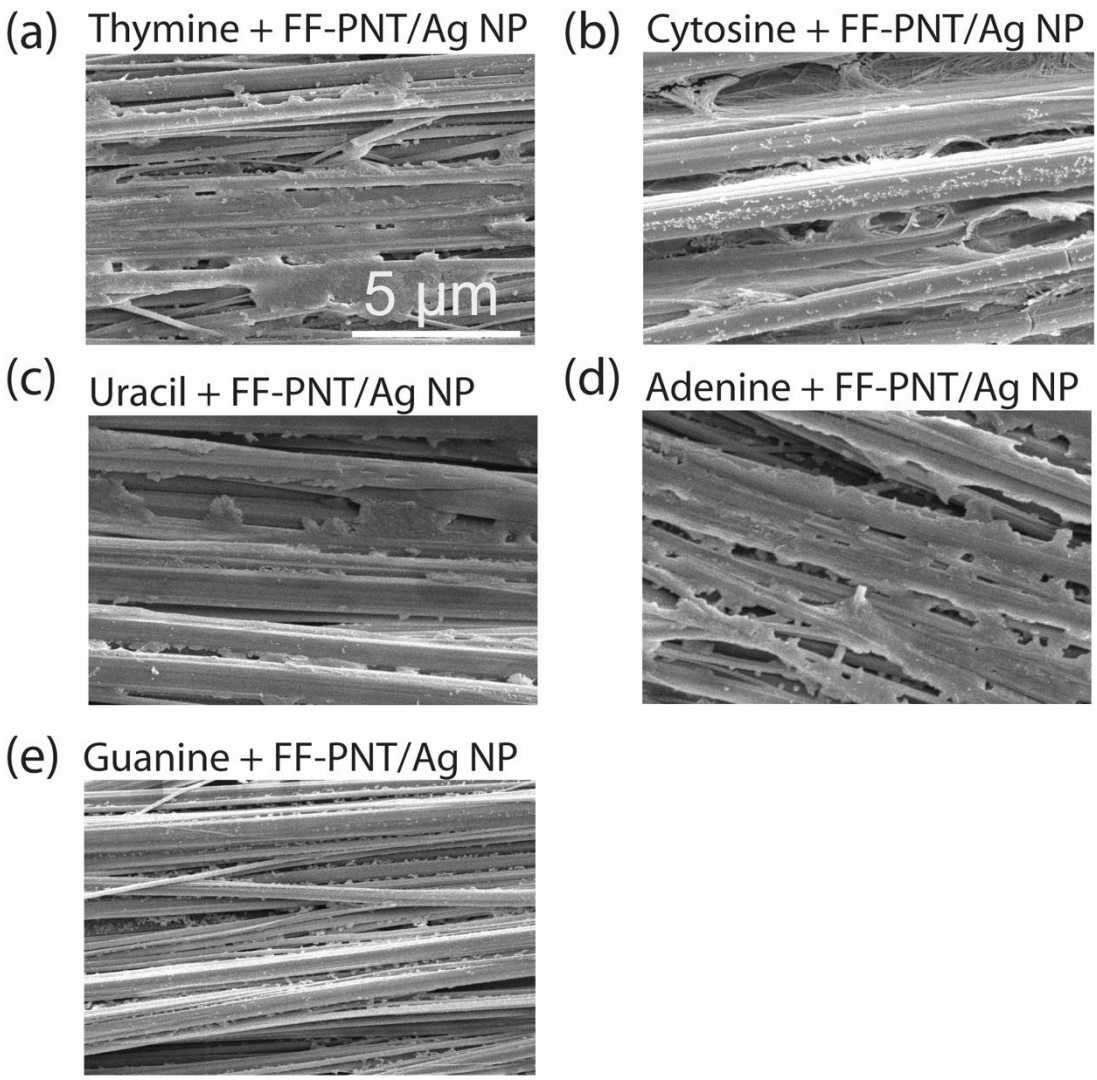

Figure 3. *SEM images of FF-PNT/Ag NP templates with (a) thymine, (b) cytosine, (c) uracil, (d) adenine, and (e) guanine, respectively, at concentrations of* 10^{-5} *M.*

To investigate the sensitivity of the FF-PNT/Ag NP template, SERS was recorded for thymine, cytosine, uracil, adenine, and guanine on the template at low concentrations (10^{-9} and 10^{-10} M). Raman intensity blinking with large variations in both Raman peak intensities and positions over time are shown in Fig. 4. Blinking is typically described as containing both a thermally-activated and an optically-induced component, meaning that it can occur as a result of thermally activated diffusion of individual or single molecules on the surface of nanoparticles coupled with photo-induced electron or charge transfer.[36–38] The observed blinking behavior using the FF-PNT/Ag NP template is a strong indication of the presence of "hot spots" (highly localized electromagnetic field due to closely packed nanoparticles) that could result from densely arranged Ag NPs. It can also can be an indication of possible charge transfer processes in the system that further increase the sensitivity of detection down to the single molecule level.[6,7,35]

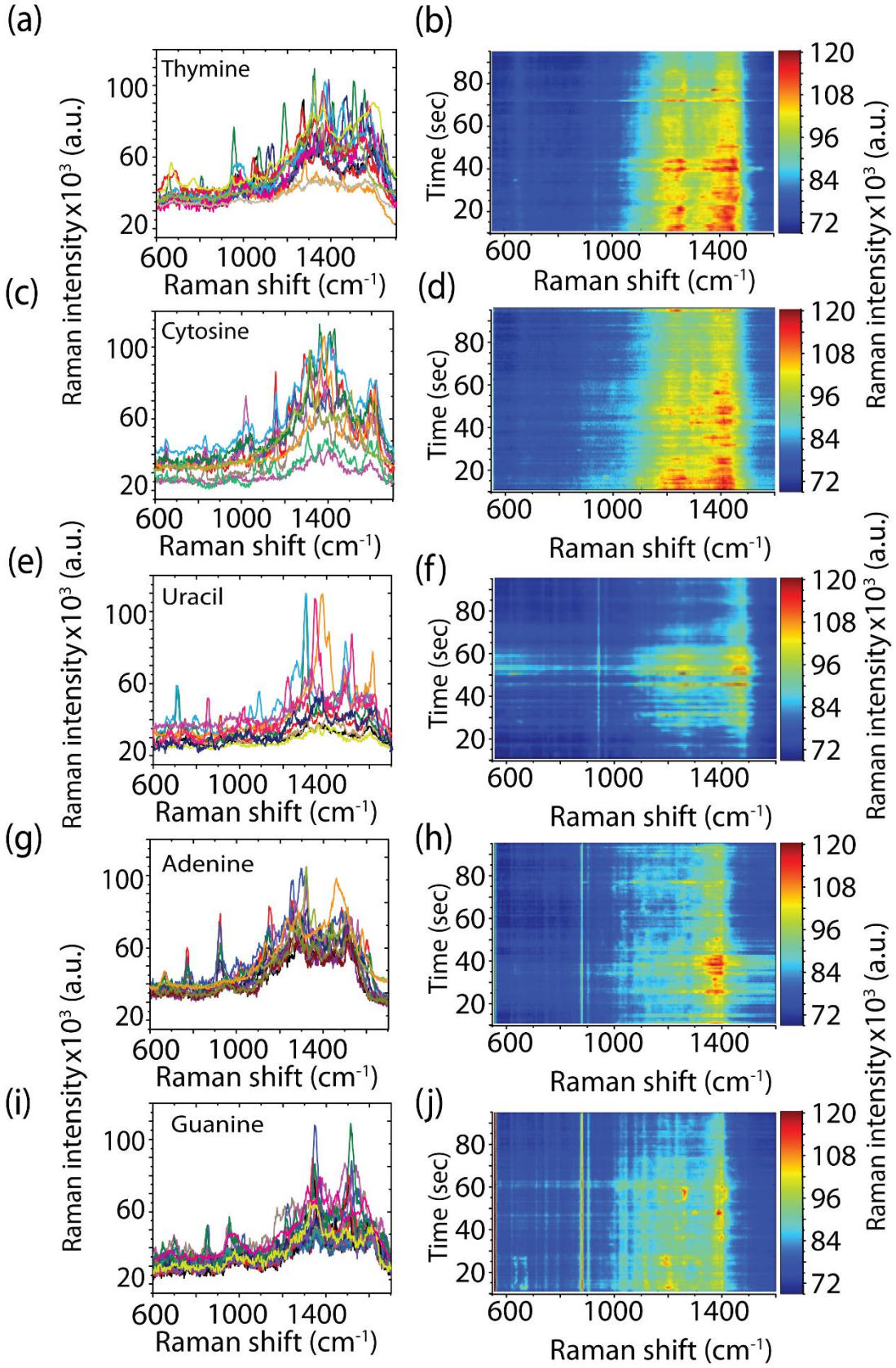

Figure 4*. Single molecule SERS spectra and contour plots showing spectral intensity fluctuations (blinking) recorded for (a, b) thymine, (c, d) cytosine, (e, f) uracil, (g, h) adenine, and (i, j) guanine on aligned FF-PNT/Ag NP templates, respectively, at a concentration of* 10^{-9} *M and with a laser power of 8 mW.*

For thymine and cytosine, 500 frames of SERS spectra were recorded over time in order to extract the time durations for the SERS ON state (when the signal is blinking on), which were then presented as log–log plots (Fig. 5a, c). Linear fits, indicative of single/few molecule SERS behavior, were made using a power law fitting function.[36–38] The SERS blinking spectra show variations in frequency, relative intensities, and line-width; however, the average SERS spectra show spectral profiles (Fig. 5b, d) consistent with the Raman spectra of the nucleobases at relatively higher concentrations (e.g., 10^{-5} M). This demonstrates that the SERS blinking arises from the nucleobases and not from sources such as decomposition products or impurities.

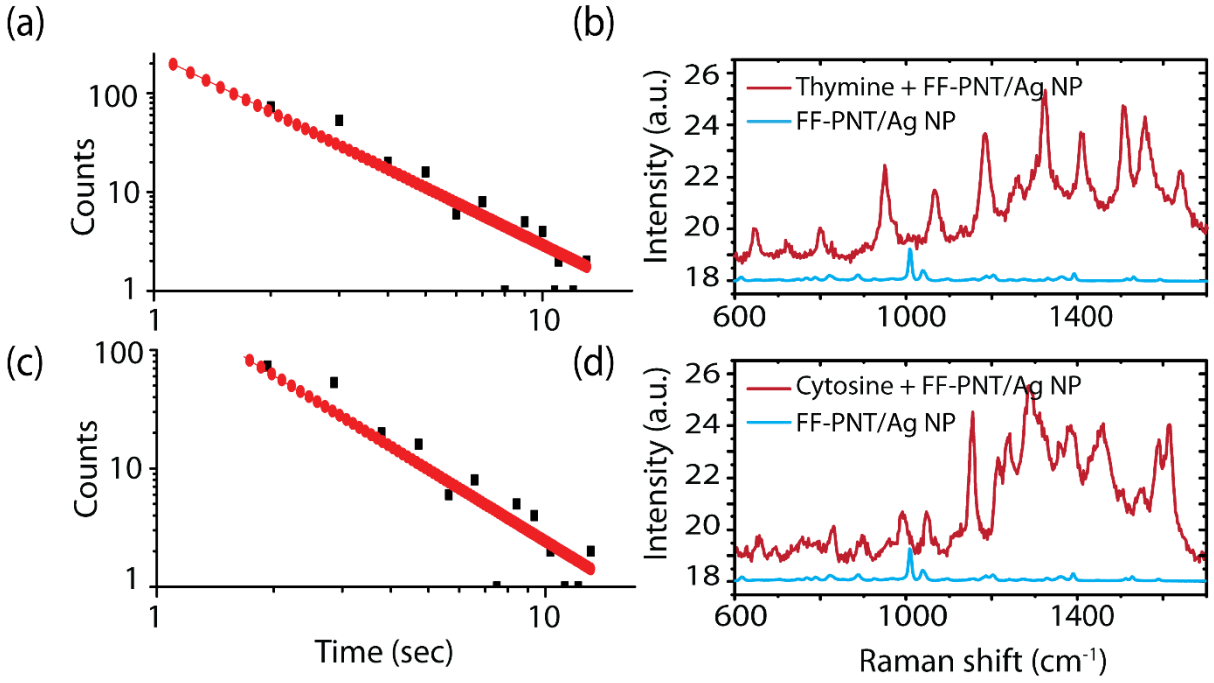

Figure 5. *(a, c) Plot of the SERS ON state (blinking on) for the thymine band at 1456 cm^{-1} and for the cytosine band at 1482 cm^{-1}, respectively; each fitted with a power law. (b, d) Average SERS spectra for thymine and cytosine, respectively, and the spectra from an FF-PNT/Ag NP template for comparison.*

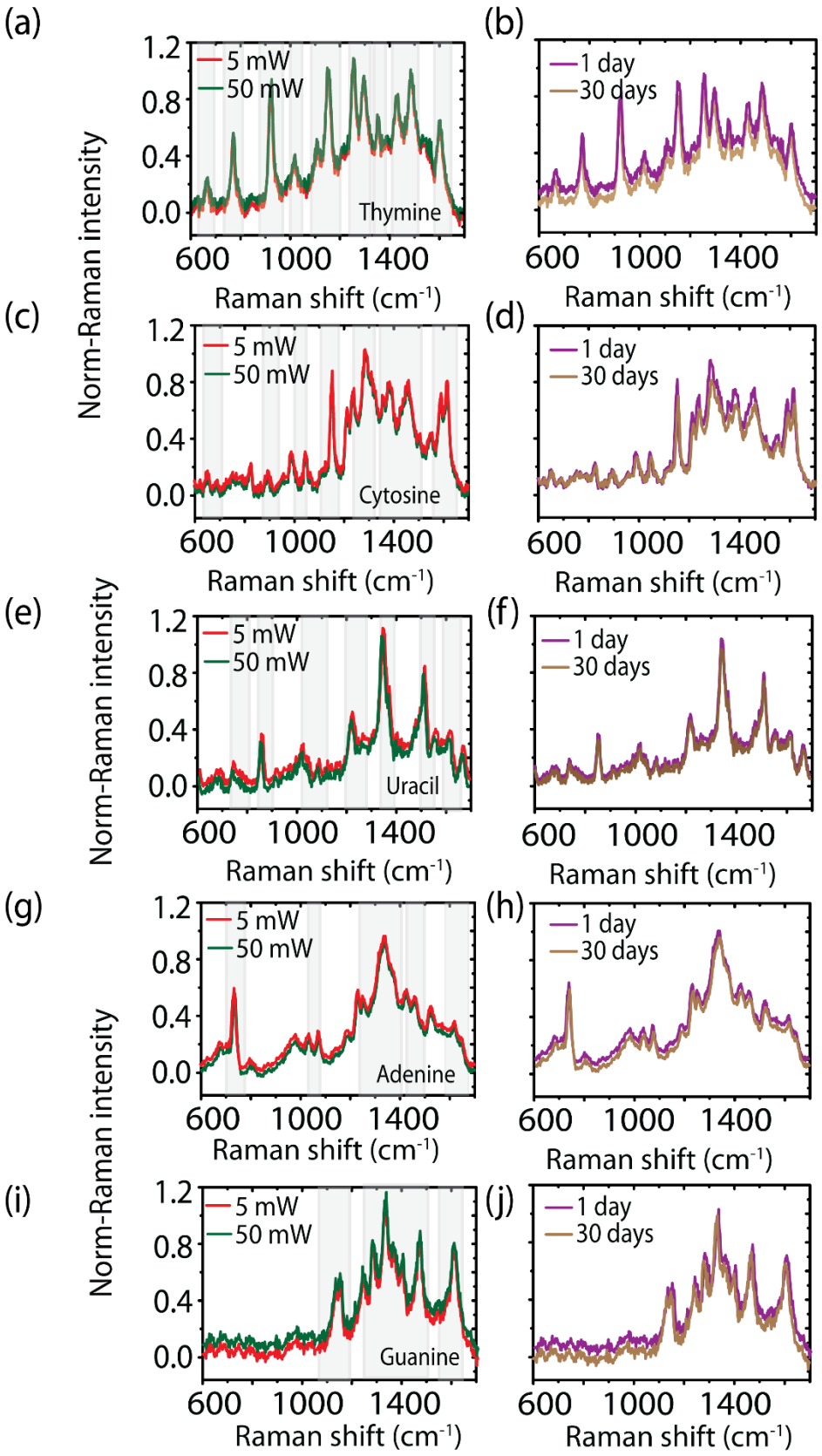

Figure 6. *SERS spectra recorded for (a, b) thymine, (c, d) cytosine, (e, f) uracil, (g, h) adenine, and (i, j) guanine, respectively, at a concentration of 10^{-4} M, showing (a, c, e, g, i) the influence of laser power (5 mW versus 50 mW) and (b, d, f, h, j) SERS signal stability over the course of 1 month.*

Stability in SERS-based sensors is crucial for practical applications. At a nucleobase concentration of 10^{-5} M, the stability of the template was demonstrated using two laser power densities, 5 mW and 50 mW for all nucleobase molecules (Fig. 6). On average, the difference in peak intensity was ~ 5.8%. This shows an absence of photodegradation of the nucleobase on these templates, in agreement with previous work for other probe molecules.[6,7] Furthermore, a decrease in peak intensity of ~ 6.4% on average was observed for the nucleobase peaks after storing the samples for 1 month (Fig. 6), illustrating the high stability of the FF-PNT/Ag NP templates.

Conclusions

We have shown that the fabricated FF-PNT/Ag NP template facilitates SERS from the nucleobases adenine, cytosine, guanine, uracil, and thymine with high sensitivity compared to control samples consisting solely of Ag NPs. This allowed the detection of all nucleobases at relatively low concentrations, e.g., 10^{-9} M. The high sensitivity of the template was attributed to several factors including: (i) the ability of FF-PNTs to densely arrange the plasmon-active Ag NPs that enhance the localized electromagnetic field; (ii) the wettability of the template or the chemical interaction with the nanotubes that facilitates the spreading of the analyte; and, (iii) the charge transfer process between Ag NPs and FF-PNTs that enhanced the chemical mechanism in SERS and hence the overall SERS intensity. The template presented here was also found to be highly stable over time, showing a decrease in SERS intensity of only around 6% over 1 month. Being able to detect nucleobases at relatively low concentrations with high stability is essential in many biomedical diagnostic schemes. These results offer a new strategy for the design of SERS-active organic semiconductor templates for ultrasensitive trace analysis to monitor biomolecules such as nucleobases.

Conflicts of interest

The authors declare that they have no competing interests.

Acknowledgements

This research was funded by the Ministry of Higher Education of Saudi Arabia under the King Abdullah Scholarship Program (ref. no. IR10161) and the European Union's Horizon 2020 research and innovation program under Marie Skłodowska-Curie grant agreement number 644175. The authors acknowledge Ian Reid for assistance with SEM, and Prof. Gareth Redmond for access to UV-Vis.

References

[1] J. Rice, R. Oliver, J. Robinson, J. Smith, R. Taylor, G. A. Briggs, M. Kappers, C. Humphreys and S. Yasin, *Phys. E Low-dimensional Syst. Nanostructures*, 2004, **21**, 546–550.

[2] S. Fedele, M. Hakami, A. Murphy, R. Pollard and J. Rice, *Appl. Phys. Lett.*, 2016, **108**.

[3] S. Damm, S. Fedele, A. Murphy, K. Holsgrove, M. Arredondo, R. Pollard, J. N. Barry, D. P. Dowling and J. H. Rice, *Appl. Phys. Lett.*, 2015, **106**, 183109.

[4] S. Damm, F. Lordan, A. Murphy, M. McMillen, R. Pollard and J. H. Rice, *Plasmonics*, 2014, **9**, 1371–1376.

[5] F. Lordan, S. Damm, E. Kennedy, C. Mallon, R. J. Forster, T. E. Keyes and J. H. Rice, *Plasmonics*, 2013, **8**, 1567–1575.

[6] S. Almohammed, S. O. Oladapo, K. Ryan, A. L. Kholkin, J. H. Rice and B. J. Rodriguez, *RSC Adv.*, 2016, **6**, 41809–41815.
[7] S. Almohammed, S. Fedele, B. J. Rodriguez and J. H. Rice, *J. Raman Spectrosc.*, 2017,**48**, 1799–1807.
[8] K. B. Andersen, J. Castillo-Leon, M. Hedström and W. E. Svendsen, *Nanoscale*, 2011, **3**, 994–998.
[9] L. Adler- Abramovich, M. Reches, V. L. Sedman, S. Allen, S. J. B. Tendler and E. Gazit, *Langmuir*, 2006, **22**, 1313.
[10] I. Bdikin, V. Bystrov, S. Kopyl, R. P. G. Lopes, I. Delgadillo, J. Gracio, E. Mishina, A. Sigov and A. L. Kholkin, *Appl. Phys. Lett.*, 2012, **100**, 043702.
[11] V. Nguyen, K. Jenkins and R. Yang, *Nano Energy*, 2015, **17**, 323–329.
[12] A. Handelman, G. Shalev and G. Rosenman, *Isr. J. Chem.*, 2015, **55**, 637–644.
[13] J. Ryu, S. Y. Lim and C. B. Park, *Adv. Mater.*, 2009, **21**, 1577–1581.
[14] H. Ma, J. Fei, Q. Li and J. Li, *Small*, 2015, **11**, 1787–1791.
[15] X. Bin, H. Y. Wang, Q. Meng, C. Yi and W. Wei, *Acta Phys. Sin.*, 2015, **64**.
[16] B. Xue, Y. Li, F. Yang, C. Zhang, M. Qin, Y. Cao and W. Wang, *Nanoscale*, 2014, **6**, 7832.
[17] G. Rosenman, P. Beker, I. Koren, M. Yevnin, B. Bank-Srour, E. Mishina and S. Semin, *J. Pept. Sci.*, 2011, **17**, 75–87.
[18] K. Komori, T. Terse-Thakoor and A. Mulchandani, *ACS Appl. Mater. Interfaces*, 2015, **7**, 3647–3654.
[19] G. Pandey, J. Saikia, S. Sasidharan, D. C. Joshi and S. Thota, *Sci. Rep.*, 2017,**7**, 1–9.
[20] M. Yemini, M. Reches, E. Gazit and J. Rishpon, *Anal. Chem.*, 2005, **77**, 5155–5159.
[21] V. V Thacker, L. O. Herrmann, D. O. Sigle, T. Zhang, T. Liedl, J. J. Baumberg and U. F. Keyser, *Nat. Commun.*, 2014, **5**, 3448.
[22] S. Kogikoski, S. Khanra, W. A. Alves and S. Guha, *J. Chem. Phys.*, 2017, **147**, 084703.
[23] A. A. Semenova, A. P. Semenov, E. A. Gudilina, G. T. Sinyukova, N. A. Brazhe, G. V. Maksimov and E. A. Goodilin, *Mendeleev Commun.*, 2016, **26**, 177–186.
[24] S. M. Li and Y. Song, *Nanoscale*, 2014, **7**, 421–425.
[25] H. Wei, S. M. Hossein Abtahi and P. J. Vikesland, *Environ. Sci. Nano*, 2015, **2**, 120–135.
[26] B. Fazio, C. D. Andrea, A. Foti, E. Messina, A. Irrera, M. G. Donato, V. Villari, N. Micali, O. M. Maragò and P. G. Gucciardi, *Nat. Publ. Gr.*, 2016, 1–13.
[27] C. Li, S. Bolisetty and R. Mezzenga, *Adv. Mater.*, 2013, **25**, 3694–3700.
[28] N. X. Dinh, T. Q. Huy, L. Van Vu, L. T. Tam and A.-T. Le, *J. Sci. Adv. Mater. Devices*, 2016, **1**, 84–89.
[29] F. Madzharova, Z. Heiner, M. Gühlke and J. Kneipp, *J. Phys. Chem. C*, 2016, **120**, 15415–15423.
[30] T.Y. Chan, T.-Y. Liu, K.S. Wang, K.-T. Tsai, Z.X. Chen, Y.C. Chang, Y.-Q. Tseng, C.-H. Wang, J.K. Wang and Y.L. Wang, *Nanoscale Res. Lett.*, 2017, **12**, 344.
[31] G. N. Ten, T. G. Burova and V. I. Baranov, 2009, **76**, 84–92.
[32] S. Almohammed, F. Zhang, B. J. Rodriguez, and J. H. Rice, *J. Phys. Chem. Lett.*, 2019, **10,** 1878–1887.
[33] R. A. Karaballi, A. Nel, S. Krishnan, J. Blackburn and C. L. Brosseau, *Phys. Chem. Chem. Phys.*, 2015, **17**, 21356–21363.
[34] V. Sereda, N. M. Ralbovsky, M. C. Vasudev, R. R. Naik and I. K. Lednev, *J. Raman Spectrosc.*, 2016, **47**, 1056–1062.
[35] S. Almohammed, F. Zhang, B. J. Rodriguez and J. H. Rice, *Sci. Rep.*, 2018, **8**, 3880.
[36] E. C. Le Ru, P. G. Etchegoin and M. Meyer, *J. Chem. Phys.*, 2006, **125**, 1–13.

[37] Y. Kitahama, Y. Tanaka, T. Itoh and Y. Ozaki, *Phys. Chem. Chem. Phys.*, 2011, **13**, 7439–48.
[38] J. R. Lombardi, R. L. Birke and G. Haran, *J. Phys. Chem. C*, 2011, **115**, 4540–4545.

TOC figure

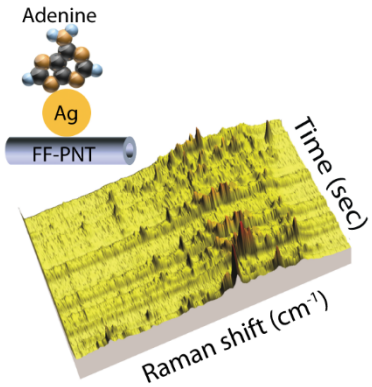

Diphenylalanine nanotube (FF-PNT) and silver nanoparticle (Ag NP) template for detection of nucleobases. The high sensitivity of the FF-PNT/Ag NP template facilitates the detection of nucleobase molecules at low concentrations.